Platelet-derived growth factor stabilises vascularisation in collagen-glycosaminoglycan scaffolds in vitro.

AUTHOR(S)

Ronaldo JFC do Amaral, Brenton Cavanagh, Fergal O'Brien, Cathal Kearney

Platelet-derived growth factor stabilises vascularisation in collagen-glycosaminoglycan scaffolds *in vitro*

Running head: Stabilisation of scaffold vascularisation by timed PDGF delivery

Ronaldo Jose Farias Correa do Amaral[a,b,c], Brenton Cavanagh[d], Fergal Joseph O'Brien[b,c,e,f], Cathal John Kearney[a,b,e,f,*]

a. *Kearney Lab, Department of Anatomy, Royal College of Surgeons in Ireland (RCSI), 123 St. Stephen's Green, Dublin 2, Ireland*
b. *Tissue Engineering Research Group, Department of Anatomy, RCSI, Dublin 2, Ireland*
c. *Centre for Research in Medical Devices (CURAM), National University of Ireland Galway, Galway, Ireland*
d. *Cellular and Molecular Imaging Core, RCSI, Dublin 2, Ireland*
e. *Trinity Centre for Bioengineering and Mechanical & Manufacturing Engineering, Trinity College Dublin, Dublin 2, Ireland*
f. *Advanced Materials and Bioengineering Research (AMBER) Centre, Dublin 2, Ireland*

** Corresponding author at: Dept. of Anatomy, Royal College of Surgeons in Ireland, 123 St. Stephen's Green, Dublin 2, Ireland.*
E-mail address: cathalkearney@rcsi.ie (C.J. Kearney).

ABSTRACT (max 250 words)

Collagen-glycosaminoglycan (CG) scaffolds have been widely developed for a range of regenerative medicine applications. To enhance their efficacy, CG scaffolds have previously been pre-vascularised *in vitro* using human endothelial cells and mesenchymal stromal cells (hMSC); however, at later time-points, a regression of vascularisation is observed. This is undesirable for longer pre-culture periods (e.g., for partial/full organ regeneration) and for *in vitro* vascularised tissue model systems (e.g., for drug testing/modelling). We hypothesised that delayed platelet-derived growth factor-BB (PDGF) addition could stabilise vessels, preventing their regression. In 2D, we identified 25ng/ml as a suitable dose that enhanced hMSC metabolic activity and proliferation, without affecting endothelial cells, or migration in either cell type. In our 3D model of CG scaffold vascularisation, early addition of PDGF (day 3), behaved similarly to no PDGF controls. However, PDGF addition at later time-points (i.e., day 4 and 5) with a second addition on day 10, prevented vascular regression. In quantifying our observations, we identified a need for a tool to measure in vitro vascularisation in porous scaffolds. This was a second key objective of this work. A novel ImageJ macro was developed, which allowed us to analyse vessel-like structures, evaluating their number and morphology, and confirmed our qualitative observations. Finally, upregulation of angiogenic genes (ANG1, KDR and TEK2) involved in vessel maturation illustrated how PDGF addition contributed to vascular stability. Taken together, the results suggest that addition of PDGF at specific time-points can be used to stabilise vasculature in CG scaffolds.

This article has been accepted for publication and undergone full peer review but has not been through the copyediting, typesetting, pagination and proofreading process which may lead to differences between this version and the Version of Record. Please cite this article as doi: 10.1002/term.2789

KEYWORDS

Collagen- based scaffolds
Vascularisation
Co-culture models
Platelet-derived growth factor
Vascularisation imaging analysis

INTRODUCTION

Effective integration of a tissue engineered construct within host tissue is dependent on host vessel ingrowth in the construct, which is a natural response to porous implanted biomaterials. This connection with the host vasculature is crucial to provide the construct with oxygen and nutrients in order to avoid necrosis in central areas of the implant (Rouwkema and Khademhosseini, 2016). Indeed, tissue engineered constructs are typically too large to rely on the diffusion alone *in situ* (Jain*, et al.*, 2005) and if vascularisation of the construct takes too long, implant survival is impaired. One strategy to enhance the integration of the implanted construct within the host circulation is to pre-vascularise the constructs prior to implantation (Laschke and Menger, 2016). The pre-formed vessels within the construct can then anastomose with the host vasculature, accelerating the process of perfusion from the host circulatory system. In order to pre-vascularise a tissue engineering construct, endothelial and mural cells (or precursors) can be cultivated *in vitro* generating a relatively stable and mature microvasculature. Pre-vascularised implants have already been shown to successfully perfuse with host vasculature, remaining stable for long periods after in vivo implantation (Chen*, et al.*, 2009, Koike*, et al.*, 2004, Levenberg*, et al.*, 2005).

Porous collagen-glycosaminoglycan (CG) biomaterials have shown high biocompatibility, high porosity, homogenous pore size distribution and are biodegradable with non-toxic degradation products (Brougham*, et al.*, 2017). Despite their success application, these scaffolds can suffer from core necrosis after implantation in vivo in certain applications (Lyons*, et al.*, 2010). This motivated the development of pre-vascularisation strategies for these porous collagen scaffolds (Duffy*, et al.*, 2011, Lloyd-Griffith*, et al.*, 2015, McFadden*, et al.*, 2013). This has been performed by co-culture of endothelial cells with mural cells, such as human mesenchymal stromal cells (hMSC) (Duffy*, et al.*, 2011, McFadden*, et al.*, 2013) or amniotic fluid-derived stem cell (AFSC) (Lloyd-Griffith*, et al.*, 2015). In these studies, a delayed addition of hMSC was advantageous (versus immediate addition), resulting in more mature vessel-like structures. Nevertheless, a regression of these vascular structures was observed after 10 days of culture (McFadden*, et al.*, 2013). Since the addition of hMSC in that system correlated with a decrease in PDGF production (McFadden*, et al.*, 2013), and PDGF is associated with vessel maturation through mural cells attraction and interaction with endothelial cells, we hypothesised that the addition of PDGF would help stabilise vascular structures for longer periods in the CG scaffolds (i.e., maintain formed vessels and prevent regression). A long-term maintenance of this in vitro engineered vascular network could be beneficial - not only for future in vivo implantation - but also as a strategy to develop novel long-term in vitro vascularised tissues and to perform long-term co-cultures of vessels and other cell & tissue types (e.g., for partial/full organ regeneration). For instance, long-term in vitro vascularisation models in porous scaffolds might be used for drug testing. Co-culture with other cell types in which the presence of vessel-like structures is important for their physiology, such as osteoblasts (mimicking a bone

marrow niche), beta cells (mimicking an islet niche), and even cancer cells (mimicking a tumour niche) would also require longer in vitro cultures. Therefore, the first objective of this work was to evaluate the effect of PDGF addition on vascular stability inside CG scaffolds.

In developing these models, we found few references that describe how to quantify/score vascular formation inside *porous* biomaterials. Some software has been used in an effort to develop more automated methodologies to quantify vessel formation in biomaterials, such as AngioTool, MATLAB, AxioVision, NIS-Elements, Scion Image, MetaMorph and the Angiogenesis Analyzer for ImageJ. Although these offer many advantages, some are not available open-source and others are more applicable to quantifying well-developed, interconnected networks of homogenous tubular structures in hydrogels (i.e., not in porous scaffolds). Qualitative analysis may be acquired with semi-quantitative scoring of microscopy images (Freiman*, et al.*, 2016) and manual quantification of vessel structures may be very time-consuming. Therefore, a secondary objective of this work was to develop a novel free ImageJ macro that is capable of detecting and analysing tubular structures among non-vessel elements in porous scaffolds.

MATERIALS AND METHODS

Cells culture

Human MSCs (hMSC) were isolated from bone marrow aspirates obtained from the iliac crest of normal human donors 20-30 years old (Lonza Biologics PLC) according to a previously established protocol (Barreto*, et al.*, 2017). Human umbilical vein endothelial cells (HUVEC) were commercially acquired (pooled, CC-2519; Lonza Switzerland). Cells were cultured in standard tissue culture flasks at 37°C under humidified atmosphere (5% CO_2 and 95% relative humidity). hMSC growth medium corresponded to low glucose Dulbecco's modified Eagles's medium (DMEM) supplemented with 10% fetal bovine serum (FBS; Hyclone) and 1% penicillin/streptomycin (Sigma–Aldrich, Ireland). HUVEC growth medium corresponded to EGM-2 media (Lonza, Switzerland). Medium was replaced every 3 days and upon reaching 80–90% confluency, cells were passaged using trypsin–EDTA solution. For the following experimental analysis cells were used up passage 6.

Scaffolds fabrication

Collagen-glycosaminoglycan (CG) scaffolds were fabricated as previously described, with minor modifications (McFadden*, et al.*, 2013). Briefly, a CG suspension was produced by blending micro-fibrillar type I bovine tendon collagen (Integra Life Sciences, Plainsboro, NJ) with chondroitin-6-sulphate, isolated from shark cartilage (Sigma–Aldrich, Germany) in 0.05 M acetic acid. The suspension was degassed at room temperature and freeze-dried at a final freezing temperature of -10°C, which was maintained constant for 60 min. The ice phase was then sublimated under vacuum (100 mTorr) at 0 °C for 17 h, in order to obtain the scaffolds. Prior to experimental use, scaffolds were cut using a biopsy punch, resulting in discs of 4 mm x 6 mm, which were chemically crosslinked using 1-ethyl-2-(3-dimethylaminopropyl) carbodiimide (EDAC) in combination with N-hydroxysuccinimide (NHS) as previously described [23]. Scaffolds were then sterilised in 70% ethanol and stored in sterile phosphate buffered saline (PBS) prior to seeding.

Metabolic activity, proliferation and migration assays

For the metabolic activity and proliferation assays, hMSC and HUVEC were seeded at a density of 1 x 10^4 cells/cm^2 and 3 x 10^4 cells/cm^2, respectively, in 24 well plate and cultured in their respective growth medium. The different cell densities were chosen based on previous experience and are due to the differences in cell size and proliferation rate. After 96h, metabolic activity was assessed by Alamar Blue assay (Thermo Fisher Scientific, Biosciences, Ireland) and proliferation was assessed by measurement of DNA content through Quant-iT PicoGreen dsDNA assay (Thermo Fisher Scientific, Biosciences, Ireland) according to manufacturer's instructions. For evaluation of cell migration, a scratch assay was performed. Briefly, hMSC and HUVEC were seeded at a density of 1.5 x 10^5 cells/cm^2 and 0.5 x 10^5 cells/cm^2, respectively, in 24 well plates and cultured in their respective growth medium. On the following day, and after observance of monolayer confluency, a scratch was performed using P20 micropipette tips. Medium was changed and cultures imaged with a Carl Zeiss AxioImager Z1 (Jena, Germany) equipped with environmental enclosure and CO_2 and hardware autofocus for 24 hours. Images were acquired every 30 minutes, and analysed with ImageJ software, from which cell front velocity was calculated. Firstly, a curve was obtained plotting the surface coverage (Y axis) per time (X axis). The slope of the linear growth phase of that curve corresponded to the centre piece approximation (% coverage/time). Then, the centre piece approximation was multiplied by the total area of the picture, and divided by the height of the picture, due to the vertical orientation of the scratch. Finally, this value was divided by 2, regarding the two cell fronts, obtaining the cell front velocity (µm/hour). To identify the effect of PDGF on cell metabolic activity, proliferation and migration, cells medium was supplemented with 0.1, 1, 10, 25 or 100ng/ml rhPDGF-BB (R&D Systems, UK).

CG scaffold 3D co-culture

Cells were seeded on each surface of the CG scaffold at a ratio of 4:1 (HUVEC:hMSC) with 5 x 10^5 cells in total (2.5 x 10^5 per scaffold side). Importantly, hMSC were added to the co-culture at day 3 after HUVEC seeding (McFadden*, et al.*, 2013). Scaffolds were cultured in 24-well suspension plates in a final volume of 1 ml medium, which comprised of complete endothelial growth media (EGM-2 media) with basic fibroblastic growth factor (bFGF), VEGF, insulin-like growth factor (IGF), ascorbic acid, epidermal growth factor (EGF), gentamycin sulphate and amphotericin-B (GA-1000), heparin (all from Lonza SingleQuots), and 2% FBS up to the first 3 days of culture, later changed to 20% FBS when hMSC were added. 500µl of medium was added on days 7 and 10, but media was not removed during culture. As noted in the experimental groups, rhPDGF (R&D Systems, UK) was added to the medium at the concentration of 25ng/ml on days 3, 4 or 5, or each added of a second supplementation on day 10. After 6, 10 and 14 days of culture, samples were separated for imaging or gene expressions analysis.

Fluorescence and imaging techniques

For fluorescence labelling, scaffolds were firstly washed in PBS and fixed in 10% neutral buffered formalin solution (Sigma-Aldrich, Ireland). After 24h fixing at 4°C, formalin solution was discharged and samples were washed with PBS. Unspecific antigen block and cells permeabilisation was performed with 0.3% triton100x (Sigma-Aldrich, Ireland) + 3% FBS in PBS for 20 minutes. Afterwards, cells cytoskeleton was stained using phalloidin TRTC (Sigma) at 1:600 diluted in PBS for 20 minutes. Monoclonal mouse Anti-Human CD31 antibody (Dako, M0823) diluted at 1:50 in PBS + 1% bovine serum albumin (BSA) and rabbit polyclonal to alpha smooth muscle actin (αSMA) antibody (Abcam,

ab5694) diluted at 1:100 in PBS + 1% BSA were also used to detect HUVEC and hMSC respectively. Primary antibodies were incubated at 4°C overnight. Rat anti-Mouse IgG (H+L) Secondary Antibody, FITC (eBiosciences, 11401185) diluted at 1:100 in PBS + 1% BSA and Goat anti-Rabbit IgG (H+L) Cross-Adsorbed Secondary Antibody, Alexa Fluor 633 (Invitrogen, A-21070) diluted at 1:400 in PBS + 1% BSA were used as secondary antibodies. Secondary antibodies were incubates for 1 hour at room temperature. For nuclei staining, Hoechst 33258 at 1:10000 diluted in PBS was added for 5 minutes. Samples were then sliced in half and observed transversely using a Carl Zeiss LSM 710 confocal microscope equipped with either a W Plan-Apochromat 20x (N.A. 1.0) or W N-Achroplan 10x (N.A. 0.3) objective. To avoid inconsistencies in the cut surface of the scaffold each Z stack image was acquired 30 µm below the surface to yield a 150 µm total depth. One central and two peripheral images were acquired per sample. Fluorender 2.21 (Wan*, et al.*, 2012) was used to visualise data in 3D and to generate complex renders of the data.

Quantification of vessel-like structures

We semi-quantitatively scored blood vessel development as previously described, with minor modifications (Freiman*, et al.*, 2016). Ranging from 0% to 100%, in which 0% corresponded to randomly dispersed cells and 100% corresponded to several tubular-like structures, evidencing maximum development, images were scored. From the 3 images acquired per sample, an average was obtained as the sample score for vessel development. With a minimum of n=3 samples per treatment, the samples scores were then averaged and statistically analysed.

The quantification of vessel length in a semi-automated manner was accomplished using a script written in the ImageJ Macro language. Briefly, the actions performed were; initialisation of the image, thresholding, conversion to a binary image, identification of objects, manual filtering of objects of interest, saving of resultant data and finally clearing the workspace for a new image. The macro is available as supplementary material (supplementary material 1). The feret diameter and area was measured to give the approximate size and length of structures of interest.

Gene expression analysis

For gene expression analysis, total RNA was isolated using an RNeasy kit (Qiagen, Crawley, UK) according to the manufacturers' instructions. Complementary DNA (cDNA) was synthesised by reverse transcription of 200 ng of total RNA using a QuantiTect reverse transcription kit (Qiagen) on a thermal cycler (Mastercycler Personal; Eppendorf, Stevenage, UK). A QuantiTect SYBR Green PCR Kit (Qiagen) was used for the quantitative real-time polymerase chain reactions (qPCR), which were run on 7500 real-time PCR System (Applied Biosystems, Paisley, UK). The mRNA relative expression was calculated by $2^{-(\Delta\Delta Ct)}$ method (Livak and Schmittgen, 2001), in which samples without PDGF addition were used as control. Target mRNA analysed were ANG1, KDR, and TEK2, with GAPDH used as a housekeeping gene.

Statistical analysis

To assess statistical difference between groups, one-way ANOVA with Bonferroni post-hoc testing was performed to compare with the control group. Significance was determined using a probability value of $p < 0.05$. All experiments were carried out with a sample size of at least 3.

RESULTS

HUVEC and hMSC proliferation and migration in 2D

In order to identify the PDGF concentration to be used in the 3D studies, we first tested the effect of PDGF dose on HUVEC and hMSC metabolic activity, proliferation and migration in 2D. Addition of PDGF in the range of 0.1 to 100 ng/ml had small – albeit significant – effects on HUVEC whole culture metabolic activity only at 10 ng/ml and 100 ng/ml (83.8% and 85.7%, respectively; see fig. 1A). When total DNA was measured (cell proliferation), no significant effect was observed (Fig. 1C). On the other hand, hMSC whole culture metabolic activity was significantly upregulated, approximately doubling versus control values after treatment with 10 ng/ml and 25 ng/ml PDGF (179% and 172% metabolic activity, respectively) (Fig. 1B). A similar result was observed on hMSC proliferation, where significant values ($p < 0.05$) at least 3 times higher than the control were observed after treatment with 10 ng/ml, 25 ng/ml and 100 ng/ml PDGF (Fig. 1D). Interestingly, when metabolic activity data was normalised to DNA quantification, it was clear that there was no detrimental effect on HUVEC metabolic activity per cell (Fig. 1E) as it has been observed on non-normalised values of the entire culture (Fig. 1A). Moreover, the normalisation of hMSC metabolic activity to DNA (Fig. 1F) evidenced that the increase in hMSC culture metabolic activity (Fig. 1A) was due to an increase in cell proliferation (Fig. 1D), since normalised values showed that increasing PDGF-BB concentration, which causes increase in cell proliferation, reduced metabolic activity/DNA (Fig. 1F). When cell migration was recorded, PDGF had no effect on HUVEC (Fig. 1G) or on hMSC (Fig. 1H). Based on the observations that 25 ng/ml PDGF had no detrimental effect over HUVEC, while it induced higher hMSC proliferation, it was selected for 3D studies.

Formation of vessel-like structures in CG scaffolds

First, we characterised vessel structures in our co-culture model using confocal microscopy. It was possible to identify diverse, heterogeneous and ramified tubular-like structures (Fig. 2A) with evidence of lumen formation both by stack visualisation (Fig. 2B) and 3D reconstruction (Fig. 2C; a video of the 3D reconstruction can be visualised as supplementary material 2). Additionally, it is possible to observe that vessel structures formed within CG scaffold pores and that the cells were not simply lining the pores (Fig. 2D). Moreover, regions with no tubular-like structures were rich in hMSC (Fig. 2D). On the other hand, the tubular-like structures were characterised by lining HUVEC with hMSC in direct contact (Fig. 2E) or in close proximity (Fig. 2F). We note, as previously observed (Lu*, et al.*, 2004), that HUVEC stained positive for CD31 and αSMA, so we used absence of CD31 stain, combined with positive αSMA as a marker of hMSC.

PDGF delayed addition avoids vessel regression in CG scaffolds

Confocal images generally suggested the development of vessel structures that can be observed at day 6 and day 10 (see exemplary images in figure 3) with and without PDGF. However, without PDGF, a regression in the vessel development is observed at day 14. Furthermore, a second addition of PDGF at day 10 for the Day 4 and Day 5 group appears to enhance the vascularisation at day 14.

Based on previous work from Freiman et al. (Freiman*, et al.*, 2016), we developed a semi-quantitative method for scoring vessel development in these images (Fig. 4A). Additionally, we developed an ImageJ macro to obtain a more automated system of vessel structure characterisation that allowed us to identify vessel structures and quantify their number, area and ferret (Fig. 4B).

Through this macro, it is possible to threshold structures in a confocal image, convert it to a binary image, identify and select vessel-like structures and analyse them (e.g. number, area and ferret).

To quantify the changes in vascular structure development, we plotted each group as a function of time of analysis (Fig. 5). From the control group, it is possible to observe an increase in vessel development (achieved by the qualitative scoring method) and number of vessels (achieved by the quantitative method) from day 6 to day 10, following by a decrease on day 14 ($p < 0.1$, comparing number of vessels on day 10 with day 14), suggesting an increase in vascularisation up to day 10 followed by a regression afterwards. This phenomenon was not observed at all – or was observed to a much lesser extent – when PDGF was added to the co-culture at select timepoints. The exception to this was addition of PDGF on day 3, which behaved similarly to control. Moreover, when a second PDGF dose was added on day 10 of culture, the analysis on day 14 presented results more similar to the peak of vascularisation on day 10, or even induced higher vascularisation (e.g., PDGF D5 + 10 group). Regarding vessel area, vessels were significantly smaller ($p<0.05$) on day 14 comparing to day 6 in the control group, which was not observed when PDGF was added to the co-culture at days 4+10 and days 5+10.

By observing the all groups (control and PDGF addition groups) at each individual time-point (supplementary material 3), it is possible to observe more profound increases in vessel development after PDGF D4 + 10 and D5 + 10 treatment on day 14. Of note, 67% of PDGF D4 and 83% of PDGF D4 + 10 samples were above a baseline of all samples of day 14, while only 33% were in the control group (the baseline has been calculated by averaging all samples of all conditions in the particular day of analysis; dashed red line). A small increase of number of vessels was also observed on day 14 of PDGF D4 + 10, with 67% of samples above baseline, while only 33% are above baseline in the control group. For vessel morphology (i.e., area and ferret), no significant differences were observed at each individual time-point. However, large vessels (i.e., above 33000 μm^2 of area and 500µm of ferret) were found in the PDGF D4 and PDGF D4 + 10 group, corresponding to 17% (area) and 16% (ferret) of vessels, while in the control group those corresponded only to 8% (area) and 9% (ferret) of vessels. Again, addition of PDGF on day 3 resulted in parameters (vessel development, number and morphology) very similar to the control group, that only the addition of PDGF at later time-points demonstrated a trend towards being more impactful.

Molecular mechanisms of PDGF action in the co-culture system

In order to understand how the addition of PDGF influenced vessels stabilisation at the gene level, we performed qPCR to identify angiogenesis-related genes that are being modulated (Fig. 6). Indeed, addition of PDGF on day 4 upregulated the expression of ANG1 ($p < 0.1$) and TEK2 ($p < 0.05$) on day 6 compared to control. On day 10, gene expression was similar to control. Finally, ANG1, KDR and TEK2 expression were upregulated, although not statistically significant, on day 14 when PDGF was added. The upregulation of these genes, especially of ANG1 and TEK2, are indicative of vessel maturation, identifying a direct effect of PDGF addition on the cells that is contributing to vessel stabilisation.

DISCUSSION

Successful vascularisation of tissue engineered constructs is crucial for their success in regenerating damaged tissues and organs (Rouwkema and Khademhosseini, 2016). Additionally, in vitro

vascularised constructs can serve as models for vascularisation studies as well as support for long-term co-cultures of different cell types and blood vessels. Although collagen-based scaffolds have been successfully applied to numerous tissue engineering applications, core necrosis due to a lack of vascularisation has been reported (O'Brien, 2011). Co-culture strategies have been described that are capable of pre-vascularising such scaffolds (Duffy*, et al.*, 2011, Lloyd-Griffith*, et al.*, 2015, McFadden*, et al.*, 2013); however, currently reported techniques result in a regression of vessels from 10 to 14 days of culture (McFadden*, et al.*, 2013). Since PDGF is known for inducing vessel maturation through recruitment of mural cells (Abramsson*, et al.*, 2003, Betsholtz, 2004, Bjarnegård*, et al.*, 2004, Hirschi*, et al.*, 1998, Lindblom*, et al.*, 2003), we hypothesised that its addition could stabilise vessels, i.e. avoid the regression of vessels grown in CG scaffolds. Identifying conditions that allow for longer maintenance of vascular structures in vitro would have applications in vascularised constructs requiring longer pre-culture periods (i.e., allowing for potential partial/whole organ regeneration) or for in vitro vascularised tissue models that could be used as model systems (e.g., drug testing). Furthermore, identifying the timing of PDGF delivery could give insight into suitable time and doses for in vivo delivery systems.

In this work, we identify conditions capable of forming and maintaining vascular structures up to 14 days in CG scaffolds and developed tools to analyse the vascular structures. The co-culture of endothelial cells and hMSC induced the formation of vessel-like structures with heterogeneous morphology, with robust (higher calibre) and delicate (smaller calibre) areas. Such heterogeneity mimics a natural vascular bed, and even patterned vascular structures may remodel during in vitro culture or post implantation (Chaturvedi*, et al.*, 2015). The possibility of those structures consisting merely of cells lining the pre-existing pores of the scaffolds was discredited by visualisation of such vessel-like structures within the collagen network and away from the pore walls. Moreover, imaging analysis suggested that the addition of PDGF maintained vessel-like structures for longer periods in our co-culture system. To quantify this observation, firstly we used a modified semi-quantitative method previously used (Freiman*, et al.*, 2016), and we additionally developed a novel ImageJ macro presented herein (and available as an open resource). There are (non-) commercial softwares available to analyse angiogenesis and vascularisation experiments; however, those are more suitable for well-formed vascular networks, and of in vivo or ex vivo experiments, such as post-natal retinas and allantois explants (Seaman*, et al.*, 2011, Vickerman*, et al.*, 2009, Zudaire*, et al.*, 2011). The macro developed enabled us to quantify the number and the morphology of vessel-like structures formed in porous scaffolds, through analysis of confocal images of phalloidin stained samples, which can be utilised to analyse a range of in vitro porous scaffold models. Importantly, we believe that this macro (fully described in supplementary material), may be used and further validated by other groups facing similar needs to quantify vascularisation in 3D porous scaffolds.

Using these techniques, our data suggest that PDGF stabilised vessels in the scaffolds, that the timing of PDGF addition was crucial to achieving this and that this was correlated to modulation of angiogenic gene expression. We came to these conclusions by first selecting a concentration of 25ng/ml PDGF in 2D, since it was the highest concentration to induce hMSC whole culture metabolic activity and proliferation, while having little or no effect on HUVEC, and on both cells migration. When normalised to DNA levels, it was clear that positive effect of PDGF-BB whole culture metabolic activity was due to an indirect effect on cells proliferation. Although we did not use mitomycin or other inhibitors of cell division in the migration assay, it is important to highlight that it happened during a 24 hours period, which is probably too short for a possible proliferation induction to cause

an effect in migration (Kramer, *et al.*, 2013, Rodriguez, *et al.*, 2005). After all, there was no effect on cell migration in 24 hours, while there was on cell proliferation in 96 hours. Taking these in consideration, we would expect in our future 3D model that 25ng/ml PDGF addition would not harm vessel formation, although it should be therapeutically active on hMSC and, potentially, promote their role in vessel stabilisation. Indeed, it has been shown previously that PDGF upregulated hMSC metabolic activity and proliferation (Chase, *et al.*, 2010, Fierro, *et al.*, 2007, Mihaylova, *et al.*, 2018). The timepoint chosen for the 2D studies was based on previously published data (Chase, *et al.*, 2010); however, it is possible that additional effects of PDGF could be identified in these cells at other timepoints. Of note, we used HUVEC as endothelial cells. This cell type has been extensively used in in vitro angiogenesis models in the literature (Bayer, *et al.*, 2016, Freiman, *et al.*, 2016, Xiao, *et al.*, 2015) and in previous publications from our group (Lloyd-Griffith, *et al.*, 2015, McFadden, *et al.*, 2013), and remains the most studied endothelial cell type due to its availability and ease of isolation and culture (Morin and Tranquillo, 2013). Nevertheless, we acknowledge that other endothelial cell types isolated from adult donors and not umbilical vein could be explored in future iterations of this work, such as human dermal microvascular endothelial cells (HDMEC) (Cui and Boland, 2009), and human blood vascular endothelial cells (Knezevic, *et al.*, 2017), which may better mimic microvascular features.

In the porous scaffolds, the quantification analysis demonstrated that the addition of 25ng/ml PDGF on days 4 and 10 of culture increased vessel stabilisation. After 14 days of culture, these groups tended towards larger and higher numbers of vessels and more developed vascularisation. This contrasted with the control group – where PDGF had not been added – where there is a trend towards vessel regression at later timepoints. This is consistent with PDGF's known role in mural cell recruitment and vessel stabilisation (Abramsson, *et al.*, 2003, Betsholtz, 2004, Bjarnegård, *et al.*, 2004, Hirschi, *et al.*, 1998, Lindblom, *et al.*, 2003). Although our data demonstrate an important role of PDGF, our standard co-culture medium contained some growth factors (e.g., VEGF and bFGF), which may have contributed to the observed data. For example, the dual delivery of VEGF and PDGF from poly(lactide-co-glycolide) scaffolds subcutaneously implanted in rats increased scaffold vascularisation as well as induced the formation of larger and more mature vessels compared to control scaffolds without growth factors or with scaffolds delivering the growth factors separately (Richardson, *et al.*, 2001). A combination of PDGF and bFGF has also been shown to synergistically maintain vascular networks in rat and rabbit ischemic hind limb models (Cao, *et al.*, 2003). Moreover, HUVEC and hMSC coculture was treated with 20% FBS, so that effects from other serum constituents might also have played a role. Of note, our model does not lead to the formation of a fully developed vascular network. There are regions of the scaffold rich in MSC but with no tubular-like structures. Although every attempt was made to homogeneously seed scaffolds, it is possible that variations in initial seeding lead to these regions and that this is responsible for the variations observed in our vascularisation quantification analysis.

Finally, our data suggest that it is not just the addition of PDGF alone, but rather the timing of its addition that is a key parameter; addition on days 4 and 5 of culture was more beneficial than an early addition (on day 3). This is in accordance with physiological angiogenesis, where firstly vessels sprout – mainly though the action of VEGF – and are later stabilised – mainly through the action of PDGF (Carmeliet, 2003). Moreover, when PDGF was constitutively overexpressed in endothelial cells, it actually inhibited mural cell differentiation and destabilised nascent blood vessels, suggesting that a more temporally and spatially controlled expression of PDGF could overcome this phenomenon

(Au*, et al.*, 2009). These observations support the idea that a delayed addition of PDGF, when vessel-like structures are already formed and mural cells are already present, should be more effective in stabilising vessels.

Finally, we investigated the possible mechanisms through which the addition of PDGF stabilised vessels in our co-culture system. Upregulation of ANG1, KDR and TEK2 could be possible explanations. ANG1 is a stimulator of vessel growth (Suri*, et al.*, 1998), and along with its receptor TEK2, promotes vessel stabilisation (Fukuhara*, et al.*, 2010). KDR, also known as the VEGF receptor 2, is the major signal transducer for angiogenesis (Shibuya, 2011). The upregulation of ANG1 and TEK2 on day 6 of culture after PDGF addition on day 4 may explain its success in stabilising vascularisation. Additionally (although not statistically significant) ANG1, KDR and TEK2 expression were upregulated on day 14 in the PDGF-treated groups. Although the gene expression inductions here observed may explain the mechanisms by which the delayed addition of PDGF stabilised vascularisation, such inductions were of the order of 2-fold increase, and therefore too low to represent the only possible explanation. Other mechanisms may involve synthesis of extracellular components important to vessel stabilisation, such as collagen type IV (Poschl*, et al.*, 2004) and laminin (Yousif*, et al.*, 2013), which should be further investigated in the future.

Future work will attempt to overcome some limitations in the system, such as the absence of flow/perfusion in our vessel-like structures (a known stabilising mechanism). It would be interesting to see if PDGF could be used alone to maintain a stable vasculature in the absence of flow and to test much later timepoints to analyse vessels and PDGF addition. Finally, it would be interesting to investigate whether having this more stable vasculature in vitro over a longer pre-culture period influences later vascular stabilisation in vivo. In the short-term, however, this work should be useful for helping the design of other systems in which vessel stabilisation in prevascularised scaffolds are intended for in vitro modelling.

CONCLUSION

Using a co-culture system of HUVEC and hMSC (as mural cells), seeded on CG scaffolds, we have shown that an addition of PDGF at select timepoints promotes vascular stabilisation, maintaining vasculature for up to 14 days. This concept is transferrable to other scaffold and drug delivery systems where promotion of stable vasculature is desired in vivo and in in vitro model systems, where a stable vasculature is desired. Furthermore, we developed novel analytical tools to investigate the formation of vasculature inside porous scaffolds. Although not directly confirmed herein, our findings suggest that the correct temporal sequence for PDGF delivery in vivo should enhance its efficacy in pro-angiogenic strategies.

ACKNOWLEDGEMENTS

The authors would like to thank Dr. Caroline Curtin, Dr. Irene Mencía Castaño, Dr. Arlyng González Vázquez and Dr. Janice O'Sullivan for help in providing isolated hMSC. The authors also thank Dr. Carolina Garciarena for providing the Alexa Fluor 633 secondary antibody. For funding, Fergal J. O'Brien and Cathal J. Kearney acknowledge RCSI's Office of Research and Innovation Seed Fund Award (Grant no. GR 14–0963); Science Foundation Ireland (SFI) under Grant no. SFI/12/RC/2278; and the European Union for a Marie Curie European Reintegration Grant under H2020 (Project Reference 659715) and ERC Starting Grant (Proj. ref: 758064). Ronaldo J. F. C. do Amaral also

acknowldeges the financial support from Science Foundation Ireland (SFI) and the European Regional Development Fund under Grant Number 13/RC/2073 as well as from the European Union's Horizon 2020 research and innovation programme under the Marie Skłodowska-Curie grant agreement No 713690.

CONFLICT OF INTEREST STATEMENT

The authors declare no conflicts of interest.

REFERENCES

Abramsson A, Lindblom P, Betsholtz C. 2003, Endothelial and nonendothelial sources of PDGF-B regulate pericyte recruitment and influence vascular pattern formation in tumors, *The Journal of clinical investigation*, **112** (8): 1142-1151.

Au P, Tam J, Duda DG*, et al.* 2009, Paradoxical effects of PDGF-BB overexpression in endothelial cells on engineered blood vessels in vivo, *The American journal of pathology*, **175** (1): 294-302.

Barreto S, Gonzalez-Vazquez A, Cameron AR*, et al.* 2017, Identification of the mechanisms by which age alters the mechanosensitivity of mesenchymal stromal cells on substrates of differing stiffness: Implications for osteogenesis and angiogenesis, *Acta biomaterialia*, **53** (Supplement C): 59-69.

Bayer EA, Fedorchak MV, Little SR. 2016, The Influence of Platelet-Derived Growth Factor and Bone Morphogenetic Protein Presentation on Tubule Organization by Human Umbilical Vascular Endothelial Cells and Human Mesenchymal Stem Cells in Coculture, *Tissue engineering Part A*, **22** (21-22): 1296-1304.

Betsholtz C. 2004, Insight into the physiological functions of PDGF through genetic studies in mice, *Cytokine & growth factor reviews*, **15** (4): 215-228.

Bjarnegård M, Enge M, Norlin J*, et al.* 2004, Endothelium-specific ablation of PDGFB leads to pericyte loss and glomerular, cardiac and placental abnormalities, *Development (Cambridge, England)*, **131** (8): 1847.

Brougham CM, Levingstone TJ, Shen N*, et al.* 2017, Freeze-Drying as a Novel Biofabrication Method for Achieving a Controlled Microarchitecture within Large, Complex Natural Biomaterial Scaffolds, *Advanced healthcare materials*.

Cao R, Brakenhielm E, Pawliuk R*, et al.* 2003, Angiogenic synergism, vascular stability and improvement of hind-limb ischemia by a combination of PDGF-BB and FGF-2, *Nature medicine*, **9** (5): 604-613.

Carmeliet P. 2003, Angiogenesis in health and disease, *Nature medicine*, **9** (6): 653-660.

Chase LG, Lakshmipathy U, Solchaga LA*, et al.* 2010, A novel serum-free medium for the expansion of human mesenchymal stem cells, *Stem cell research & therapy*, **1** (1): 8.

Chaturvedi RR, Stevens KR, Solorzano RD*, et al.* 2015, Patterning vascular networks in vivo for tissue engineering applications, *Tissue engineering Part C, Methods*, **21** (5): 509-517.

Chen X, Aledia AS, Ghajar CM*, et al.* 2009, Prevascularization of a fibrin-based tissue construct accelerates the formation of functional anastomosis with host vasculature, *Tissue engineering Part A*, **15** (6): 1363-1371.

Cui X, Boland T. 2009, Human microvasculature fabrication using thermal inkjet printing technology, *Biomaterials*, **30** (31): 6221-6227.

Duffy GP, McFadden TM, Byrne EM*, et al.* 2011, Towards in vitro vascularisation of collagen-GAG scaffolds, *European cells & materials*, **21**: 15-30.

Fierro F, Illmer T, Jing D*, et al.* 2007, Inhibition of platelet-derived growth factor receptorbeta by imatinib mesylate suppresses proliferation and alters differentiation of human mesenchymal stem cells in vitro, *Cell proliferation*, **40** (3): 355-366.

Freiman A, Shandalov Y, Rozenfeld D*, et al.* 2016, Adipose-derived endothelial and mesenchymal stem cells enhance vascular network formation on three-dimensional constructs in vitro, *Stem cell research & therapy*, **7**: 5.

Fukuhara S, Sako K, Noda K*, et al.* 2010, Angiopoietin-1/Tie2 receptor signaling in vascular quiescence and angiogenesis, *Histology and histopathology*, **25** (3): 387-396.

Hirschi KK, Rohovsky SA, D'Amore PA. 1998, PDGF, TGF-beta, and heterotypic cell-cell interactions mediate endothelial cell-induced recruitment of 10T1/2 cells and their differentiation to a smooth muscle fate, *The Journal of cell biology*, **141** (3): 805-814.

Jain RK, Au P, Tam J*, et al.* 2005, Engineering vascularized tissue, *Nat Biotech*, **23** (7): 821-823.

Knezevic L, Schaupper M, Muhleder S*, et al.* 2017, Engineering Blood and Lymphatic Microvascular Networks in Fibrin Matrices, *Front Bioeng Biotechnol*, **5**: 25.

Koike N, Fukumura D, Gralla O*, et al.* 2004, Creation of long-lasting blood vessels, **428**: 138.
Kramer N, Walzl A, Unger C*, et al.* 2013, In vitro cell migration and invasion assays, *Mutat Res*, **752** (1): 10-24.
Laschke MW, Menger MD. 2016, Prevascularization in tissue engineering: Current concepts and future directions, *Biotechnology advances*, **34** (2): 112-121.
Levenberg S, Rouwkema J, Macdonald M*, et al.* 2005, Engineering vascularized skeletal muscle tissue, *Nat Biotech*, **23** (7): 879-884.
Lindblom P, Gerhardt H, Liebner S*, et al.* 2003, Endothelial PDGF-B retention is required for proper investment of pericytes in the microvessel wall, *Genes & development*, **17** (15): 1835-1840.
Livak KJ, Schmittgen TD. 2001, Analysis of relative gene expression data using real-time quantitative PCR and the 2(-Delta Delta C(T)) Method, *Methods (San Diego, Calif)*, **25** (4): 402-408.
Lloyd-Griffith C, McFadden TM, Duffy GP*, et al.* 2015, The pre-vascularisation of a collagen-chondroitin sulphate scaffold using human amniotic fluid-derived stem cells to enhance and stabilise endothelial cell-mediated vessel formation, *Acta biomaterialia*, **26**: 263-273.
Lu X, Dunn J, Dickinson AM*, et al.* 2004, Smooth muscle alpha-actin expression in endothelial cells derived from CD34+ human cord blood cells, *Stem cells and development*, **13** (5): 521-527.
Lyons FG, Al-Munajjed AA, Kieran SM*, et al.* 2010, The healing of bony defects by cell-free collagen-based scaffolds compared to stem cell-seeded tissue engineered constructs, *Biomaterials*, **31** (35): 9232-9243.
McFadden TM, Duffy GP, Allen AB*, et al.* 2013, The delayed addition of human mesenchymal stem cells to pre-formed endothelial cell networks results in functional vascularization of a collagen-glycosaminoglycan scaffold in vivo, *Acta biomaterialia*, **9** (12): 9303-9316.
Mihaylova Z, Tsikandelova R, Sanimirov P*, et al.* 2018, Role of PDGF-BB in proliferation, differentiation and maintaining stem cell properties of PDL cells in vitro, *Arch Oral Biol*, **85**: 1-9.
Morin KT, Tranquillo RT. 2013, In Vitro Models of Angiogenesis and Vasculogenesis in Fibrin Gel, *Experimental cell research*, **319** (16): 2409-2417.
O'Brien FJ. 2011, Biomaterials & scaffolds for tissue engineering, *Materials Today*, **14** (3): 88-95.
Poschl E, Schlotzer-Schrehardt U, Brachvogel B*, et al.* 2004, Collagen IV is essential for basement membrane stability but dispensable for initiation of its assembly during early development, *Development (Cambridge, England)*, **131** (7): 1619-1628.
Richardson TP, Peters MC, Ennett AB*, et al.* 2001, Polymeric system for dual growth factor delivery, *Nat Biotech*, **19** (11): 1029-1034.
Rodriguez LG, Wu X, Guan JL. 2005, Wound-healing assay, *Methods Mol Biol*, **294**: 23-29.
Rouwkema J, Khademhosseini A. 2016, Vascularization and Angiogenesis in Tissue Engineering: Beyond Creating Static Networks, *Trends in biotechnology*, **34** (9): 733-745.
Seaman ME, Peirce SM, Kelly K. 2011, Rapid Analysis of Vessel Elements (RAVE): A Tool for Studying Physiologic, Pathologic and Tumor Angiogenesis, *PloS one*, **6** (6).
Shibuya M. 2011, Vascular Endothelial Growth Factor (VEGF) and Its Receptor (VEGFR) Signaling in Angiogenesis: A Crucial Target for Anti- and Pro-Angiogenic Therapies, *Genes & cancer*, **2** (12): 1097-1105.
Suri C, McClain J, Thurston G*, et al.* 1998, Increased vascularization in mice overexpressing angiopoietin-1, *Science*, **282** (5388): 468-471.
Vickerman MB, Keith PA, McKay TL*, et al.* 2009, VESGEN 2D: automated, user-interactive software for quantification and mapping of angiogenic and lymphangiogenic trees and networks, *Anatomical record (Hoboken, NJ : 2007)*, **292** (3): 320-332.
Wan Y, Otsuna H, Chien CB*, et al.* FluoRender: An application of 2D image space methods for 3D and 4D confocal microscopy data visualization in neurobiology research. 2012 IEEE Pacific Visualization Symposium2012. p. 201-208.

Xiao X, Wang W, Liu D*, et al.* 2015, The promotion of angiogenesis induced by three-dimensional porous beta-tricalcium phosphate scaffold with different interconnection sizes via activation of PI3K/Akt pathways, *Scientific reports*, **5**.

Yousif LF, Di Russo J, Sorokin L. 2013, Laminin isoforms in endothelial and perivascular basement membranes, *Cell Adh Migr*, **7** (1): 101-110.

Zudaire E, Gambardella L, Kurcz C*, et al.* 2011, A computational tool for quantitative analysis of vascular networks, *PloS one*, **6** (11): e27385.

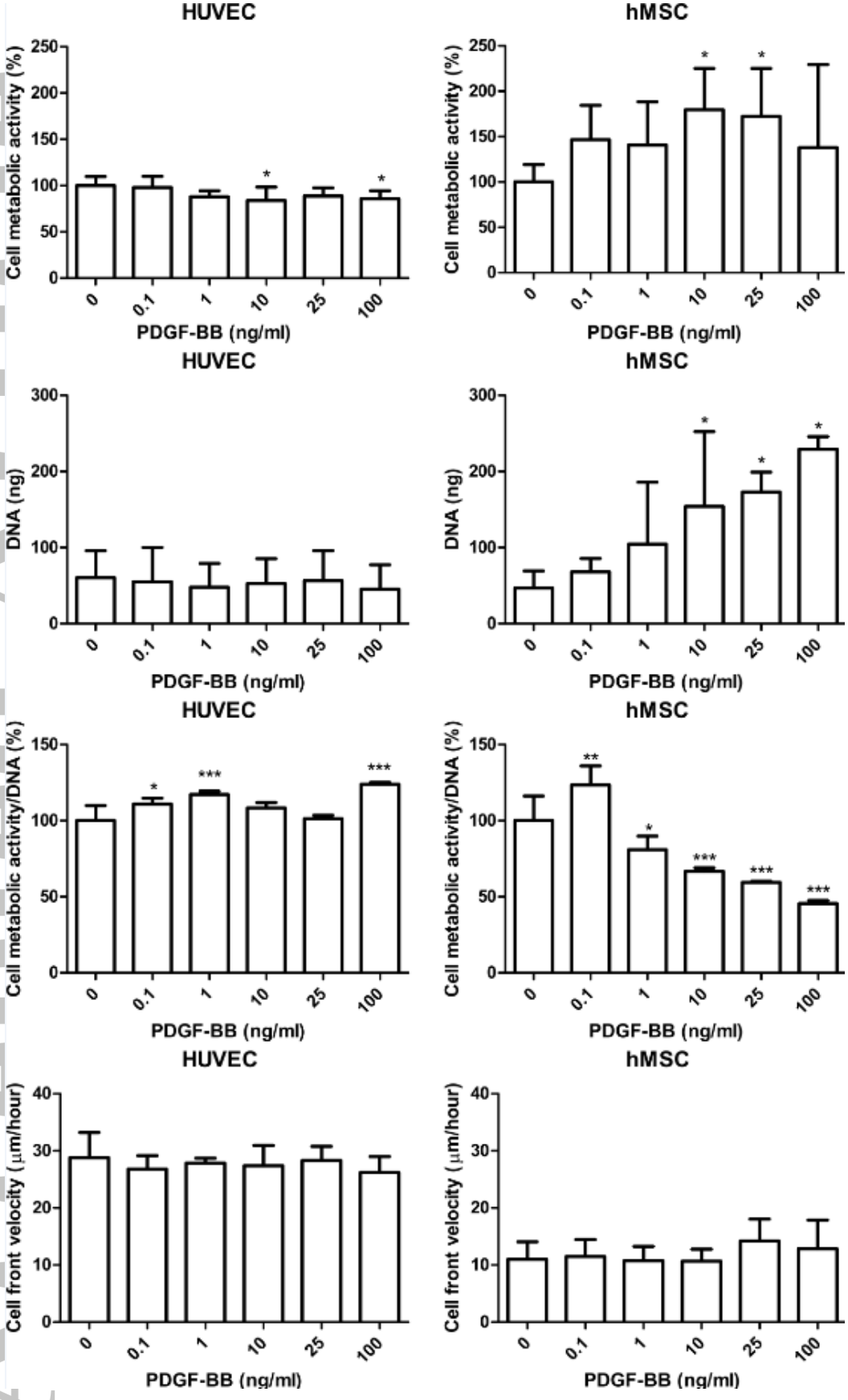

Fig 1: Effects of different concentrations of PDGF (0 - 100 ng/ml) on (A, C, E, G) HUVEC and (B, D, F, H) hMSC (A, B) metabolic activity, (C, D) proliferation, (E, F) metabolic activity normalised to DNA levels and (G, H) migration. PDGF had no or little effect on HUVEC metabolic activity (A), proliferation (C), metabolic activity/DNA (E) and migration (G). By contrast, PDGF upregulated hMSC metabolic activity (B) and proliferation (D). When normalised to DNA levels, increasing PDGF concentrations reduced hMSC metabolic activity/DNA, indicating that the increase in hMSC metabolic activity was an indirect effect on cell proliferation. No significant effect was observed on hMSC migration (H). * denotes $p<0.05$, ** denotes $p<0.01$, and *** denotes $p<0.001$. Data are expressed as mean and error bars correspond to standard deviation.

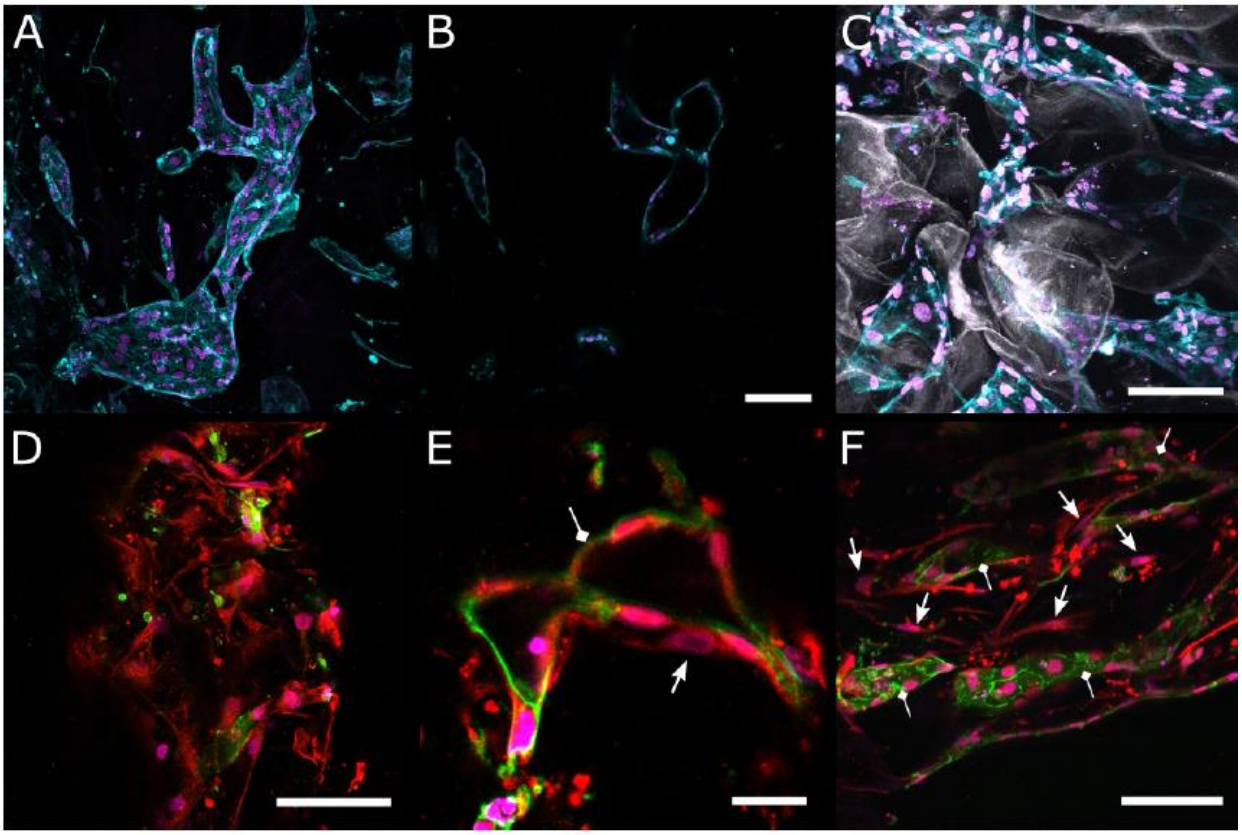

Fig 2: Vessel-like structure formation in CG scaffolds in vitro. (A) Confocal reconstitution image of 23 stacks. (B) Confocal image of a single stack from the reconstitution in (A) demonstrating lumen formation in the vessel-like structure. (C) Evidence of tubular-like formation within CG scaffolds pores. (D) Area with no tubular-like structures, rich in hMSC (αSMA stained in red). (E) Single stack of a tubular-like structure with HUVEC lining (CD31 stained in green) and hMSC (αSMA stained in red) in direct contact. (F) Confocal reconstitution image of 38 stacks with tubular-like structures with HUVEC lining (CD31 stained in green) and hMSC (αSMA stained in red) in proximity. Scale bars represent 100 µm in (B, C, D, F) and 20 µm in (E). Cell nuclei in magenta, actin cytoskeleton in cyan, collagen in white, CD31 in green and αSMA in red. Diamonds indicate HUVEC and arrows indicate hMSC.

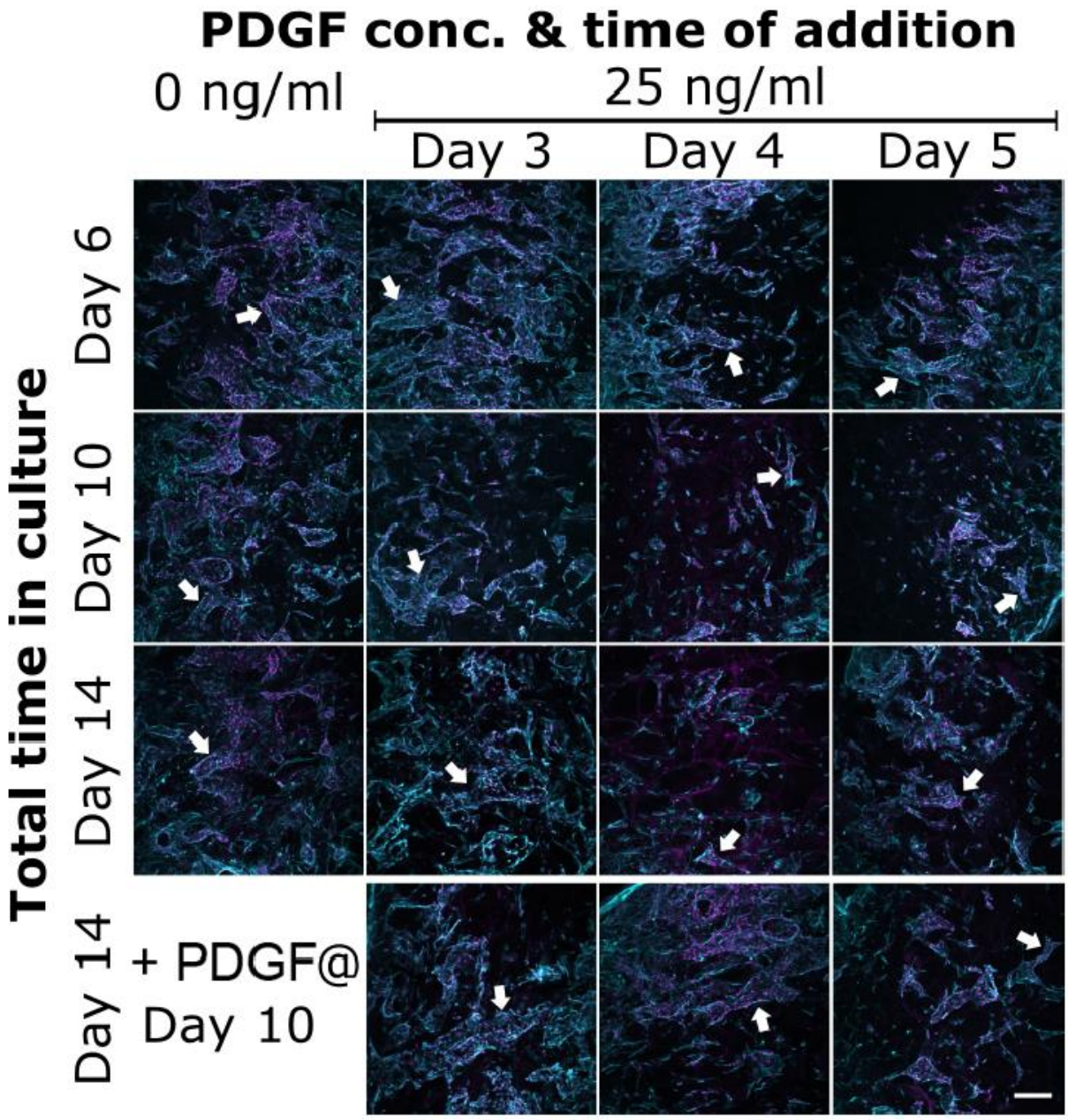

Fig 3: Exemplary confocal images of co-cultured scaffolds with and without PDGF addition as a function of time. Co-cultures were treated with PDGF at 0 ng/ml or at 25 ng/ml on days 3, 4, 5, with a second addition on day 10 as indicated. Analyses were performed after 6, 10 and 14 days in culture. Images suggest enhanced vessel-like structure formation from day 6 to day 10, with a regression on day 14. The exceptions were the groups where PDGF was added, in particular on days 4 + 10 and days 5 + 10. Scale bar represent 200 µm. Cells nuclei in magenta, actin cytoskeleton in cyan and collagen in white. White arrows indicate one example vessel-like structures in each image.

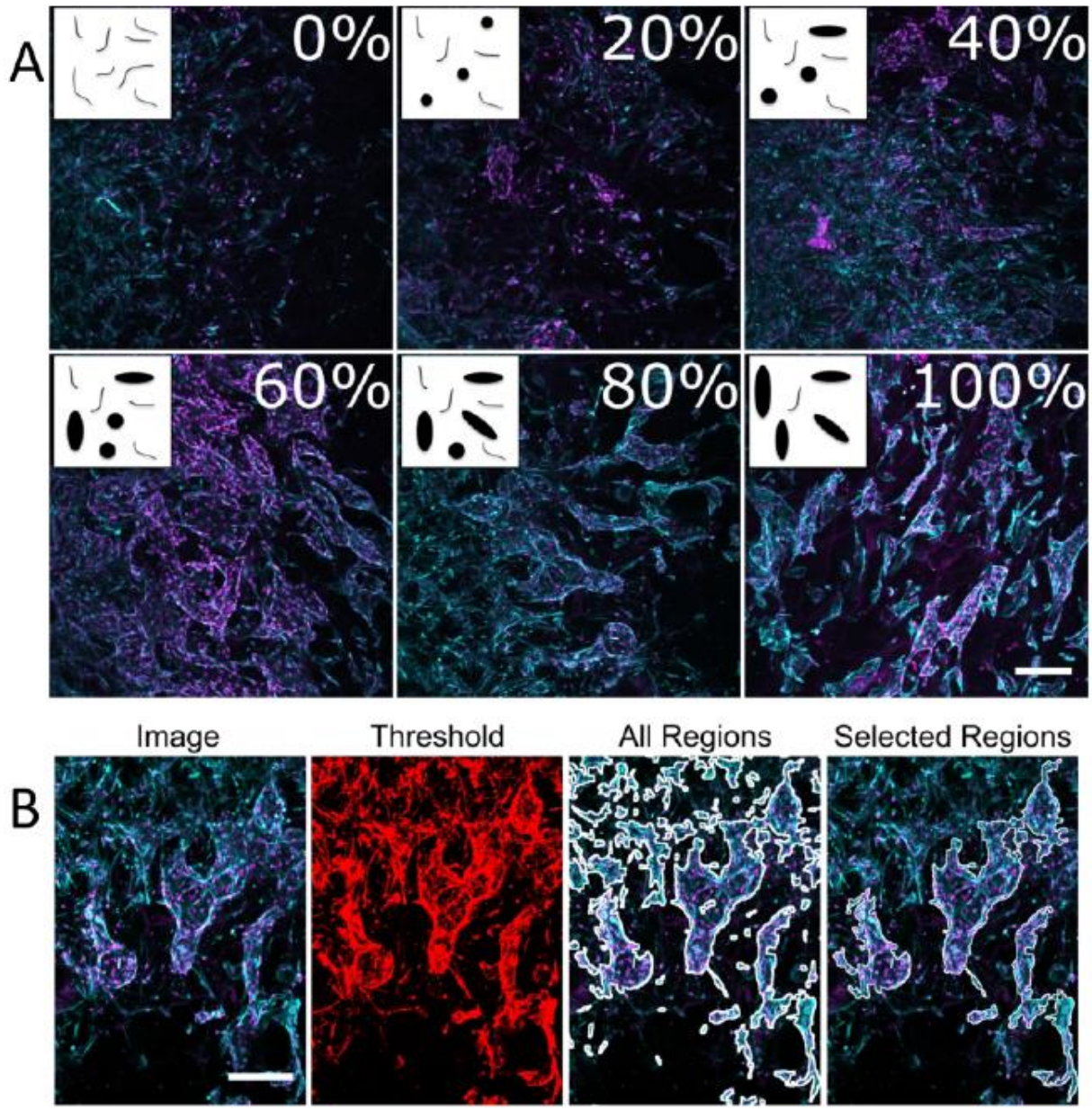

Fig 4: Quantification method for vascularisation in porous scaffolds. (A) Semi-quantitative method for scoring vessel development. Insert schematics show distributions of sparsely distributed cells (lines), cells clusters (circles) and vessel-like structures (ellipses): 0% – cells only; 20% – cells starting to organise in clusters; 40% – some elongated vessel-like structures starts to appear; 60% – mixture of cells clusters and vessel-like structures; 80% – image is mainly formed by vessel-like structures; 100% – complete vessel formation. (B) Quantitative method for analysis of vessels structures using an ImageJ macro. A threshold is applied to an image, which selects several regions of interest ("All Regions"). The user can then select the regions ("Selected Regions") corresponding to vessel-like structures, which are then quantified for their number, ferret, area.

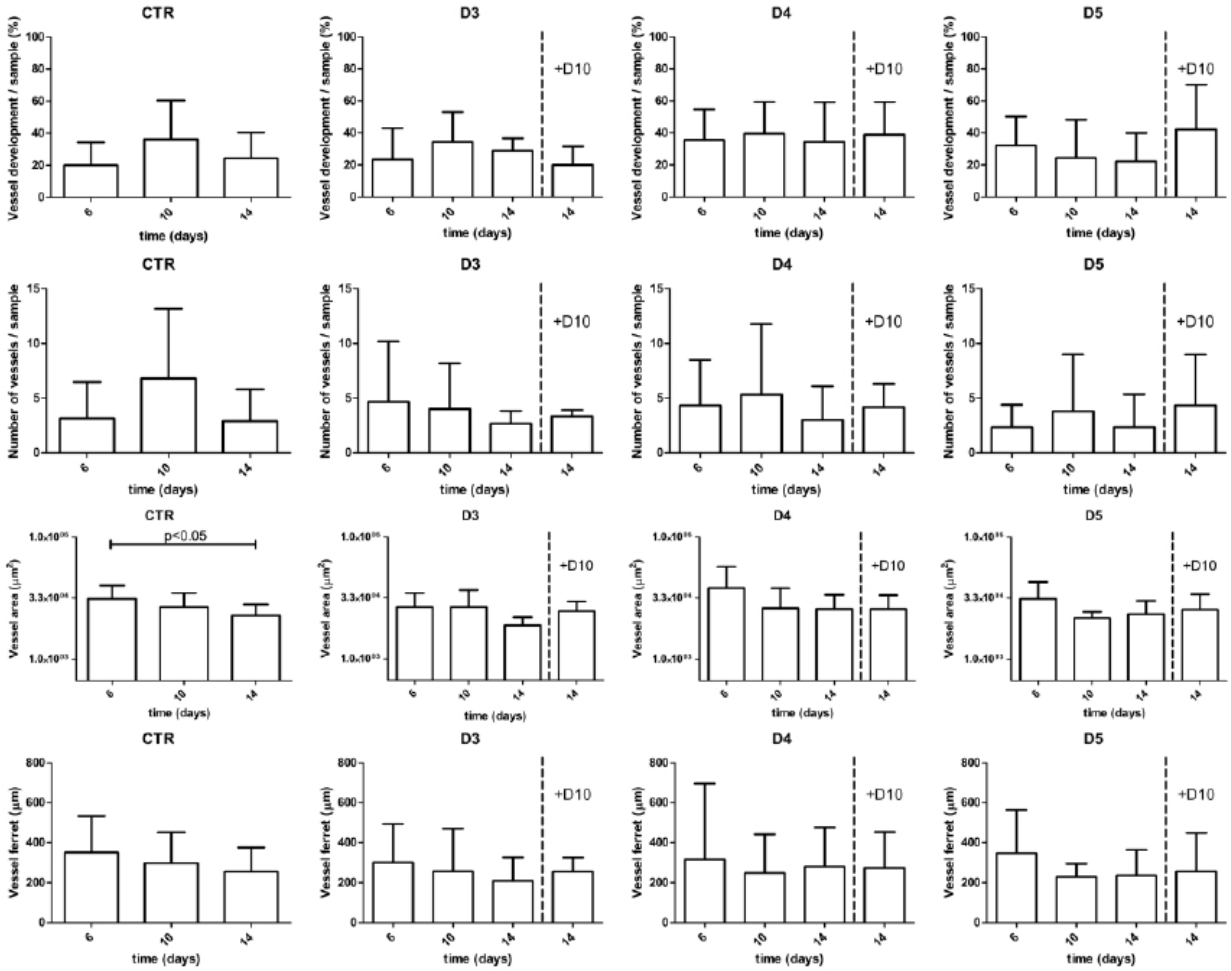

Fig 5: Quantitative analysis of vessel development, number of vessels and vessel morphology (area and ferret) for each treatment group (CTR = 0 ng/ml PDGF, 25 ng/ml PDGF added on day 3, 4 and 5, corresponding to D3, D4 and D5 respectively; in some cases there was a second addition on day 10, corresponding to +D10). Data are expressed as mean and error bars correspond to standard deviation. There was an increase in vessel development and number of vessels from day 6 to day 10, followed by a decrease on day 14 in the control group. When PDGF was added – specifically D4+10 and D5+10 – this regression was avoided. Vessel area significantly reduced from day 6 to day 14 in the control group ($p < 0.05$). * denotes $p < 0.05$.

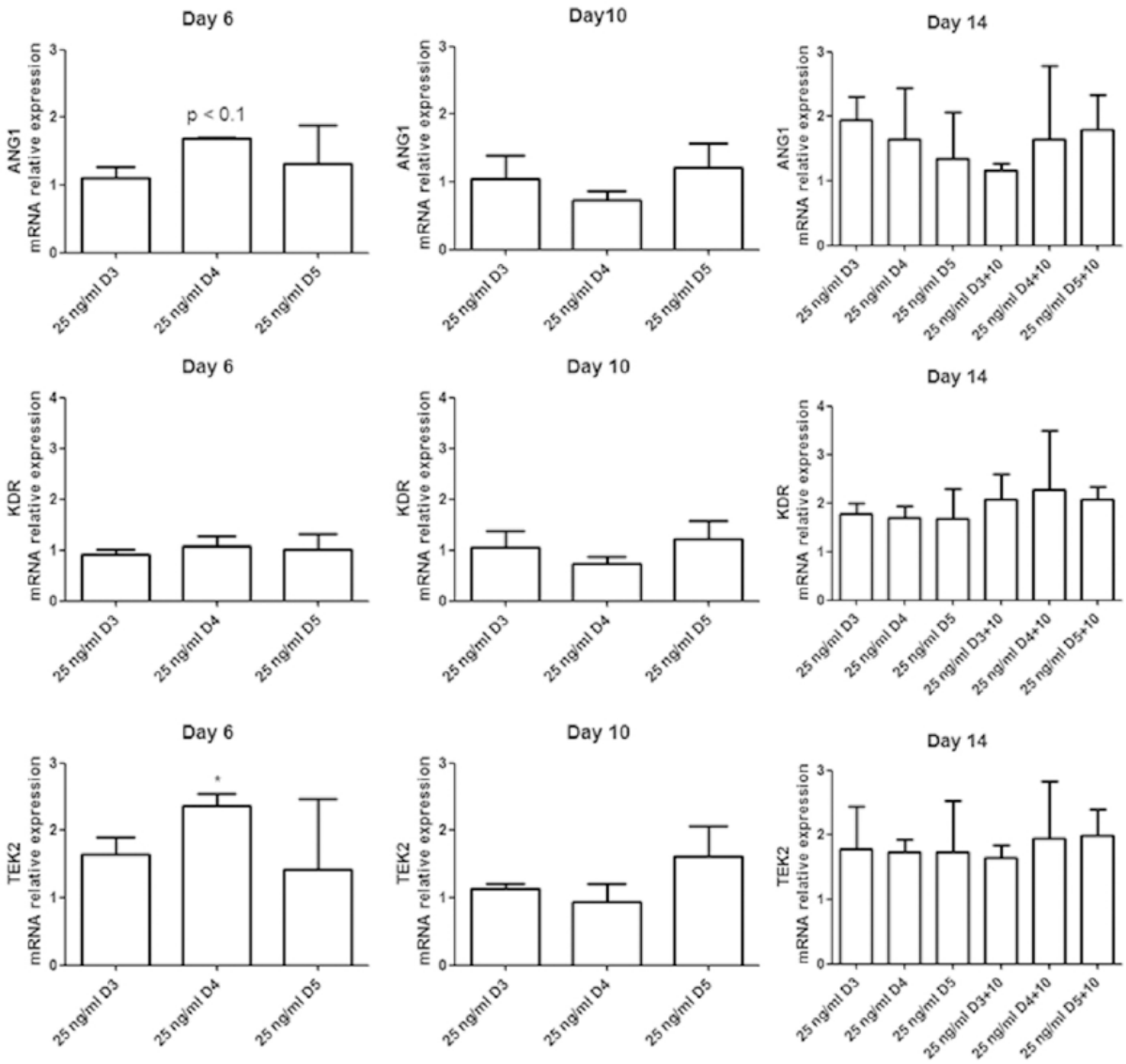

Fig 6: qPCR analysis of angiogenic gene expression after addition of PDGF to co-cultures. The upregulation of ANG1 and TEK2, which are involved in vessel maturation, on day 6 after addition of PDGF on day 4 suggests a molecular mechanism through which PDGF addition on this particular timepoint had beneficial effects on vessel stabilisation. KDR and TEK2 were also upregulated on day 14 after PDGF addition. * denotes $p < 0.05$. Data are expressed as mean and error bars correspond to standard deviation.